

## ACCELERATING PROCESS OF SURFACE-SHEARED SAND LAYER

By

Hitoshi GOTOH

Associate Professor, Graduate School of Civil Engineering, Kyoto University  
Yoshida Hon-machi, Sakyo-ku, Kyoto, 606-8501, Japan.

and

Tetsuo SAKAI

Professor, Graduate School of Civil Engineering, Kyoto University  
Yoshida Hon-machi, Sakyo-ku, Kyoto, 606-8501, Japan.

### ABSTRACT

Accelerating process of the sand layer under the action of shear stress on its surface is numerically simulated with focusing upon the particle/particle interaction. The developing process of the particle-velocity profile simulated by the distinct element method is explained as a relaxation process related to the time lag of the individual sand particle responding to the change of shear stress acting on the surface of sand layer. The accelerating process of the velocity of particle is discussed from a viewpoint of the granular-material dynamics.

### INTRODUCTION

Particle/particle interaction plays an important role in the highly concentrated sediment-laden flow, which occurs under the action of high bed-shear stress. Debris flow in a river and sediment transport in sheetflow regime in coastal region belong to this category. Most of the previous studies on the highly concentrated sediment-laden flow, or granular-material flow have treated the steady state. Hence the study on the mechanism of the developing process, or the accelerating process, of granular-material flow is not sufficient.

There are many cases in which the developing process of granular-material flow is dominant. It is necessary to estimate the length of the developing region of the flow before reaching the equilibrium state, to determine the location of the test section of debris-flow experiment, and the unsteadiness, which is one of the fundamental characteristics of the sediment transport in sheetflow regime. To understand the mechanism of these situations, it is essential to know the characteristics of the accelerating and decelerating process of granular-material flow.

Authors (1,2) performed the numerical simulation of granular-material flow based on the distinct element method (DEM) originally proposed by Cundall and Strack (3), in which the Lagrangian motion of sediment particles interacting each other is treated numerically. There have been some studies of the application of DEM to the subjects of hydraulics. Oda, Shigematsu and Ujimoto (4) performed a numerical simulation of the settling behavior of soil dumped into water by combining the DEM with the MAC method. Mishima, Akiyama and Tsuchiya (5) conducted the numerical study of grain-bed impacts in blown sand based on the DEM. They investigated numerically the distribution of the ejection velocity and angle, which are the fundamental characteristics of the collision process of the saltating grains. Haff and Anderson (6) investigated the grain dynamics in aeolian sediment transport problems by using the DEM. They reproduced the details of the grain impact process in aeolian saltation and collected the statistical information of the saltating particles affected by the bed microtopography.

In this study, the developing process of the velocity profile of sediment particles under the action of constant shear stress is simulated by applying the numerical model developed by the authors (1,2) to the accelerating process of granular-material flow. Furthermore, the mechanism of developing process of the velocity profile of particle is discussed based on the simulation data such as snapshots of the instantaneous motion of particles.

## SIMULATION MODEL

Motion of rigid cylinders are numerically traced in a vertically two dimensional plane with taking the inter-cylinder acting forces into account by introducing the spring-dashpot systems at all the contacting points between cylinders.

Equations of motion of the  $i$ -th particle in streamwise ( $x$ ) and upward vertical ( $y$ ) direction and the rotational motion of particles are as follows:

$$M \frac{d^2 x_i}{dt^2} = \sum_j \left\{ -f_n(t) \cos \alpha_{ij} + f_s(t) \sin \alpha_{ij} \right\} + F_{oi} \quad (1)$$

$$M \frac{d^2 y_i}{dt^2} = \sum_j \left\{ -f_n(t) \sin \alpha_{ij} + f_s(t) \cos \alpha_{ij} \right\} - (M - \rho V)g \quad (2)$$

$$I \frac{d^2 \phi_i}{dt^2} = r \cdot \sum_j \{ f_s(t) \} \quad (3)$$

in which  $f_n, f_s$ =normal and tangential components of the force acting between the  $i$ -th and  $j$ -th particles on the local coordinate system  $n-s$ ;  $\alpha_{ij}$ =contacting angle between the  $i$ -th and  $j$ -th particles;  $F_{oi}$ =shear force acting on the  $i$ -th particle;  $M$ =mass of particle ( $=\sigma\pi r^2$ ;  $\sigma$ =density of particle; and  $r$ =radius of particle ( $=d/2$ ;  $d$ =diameter of particle));  $\rho$ =density of fluid;  $V$ =volume of the particle;  $I$ =moment of inertia of the particle ( $=\sigma\pi r^4/2$ ); and  $g$ =gravitational acceleration.

Figure 1 shows schematically the domain of calculation. In this simulation, the streamwise uniform condition is treated, therefore, the periodic boundaries are introduced at both sides of the calculated domain. The bottom boundary is the fixed rough bed constituted by particles with the same diameter as the moving ones.

The shear stress,  $F_{oi}$ , is distributed to the particles in the neighborhood of the surface of sand layer (see Gotoh and Sakai (1), (2)). Firstly, the threshold  $y_{th}$  (= averaged elevation of surface-constituting particles) is set; secondarily the area of the particles above the threshold,  $S_{th}$ , is calculated for the particles existing on and above the threshold; and finally the shear force is distributed onto the particles existing on and above the threshold as the calculated area  $S_{th}$ . The test particle is 0.5 cm in diameter and 2.65 in specific gravity. In the calculated domain, 69 particles are located in 15 layers: there are 5 particles in each layer except the surface layer, and 4 particles exist at the surface layer for the easy initiation of the particles motion. The model constants are as follows: the spring constants  $k_n (=9.45 \times 10^6 \text{ N/m})$ ,  $k_s (=2.36 \times 10^6 \text{ N/m})$ ; the dashpot constants  $\eta_n (=40.0 \text{ Ns/m})$ ,  $\eta_s (=20.0 \text{ Ns/m})$ ; coefficient of friction force

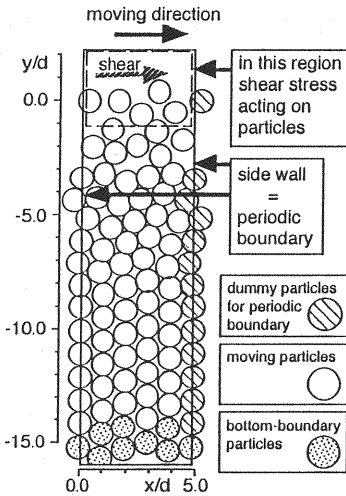


Fig. 1 Calculation domain

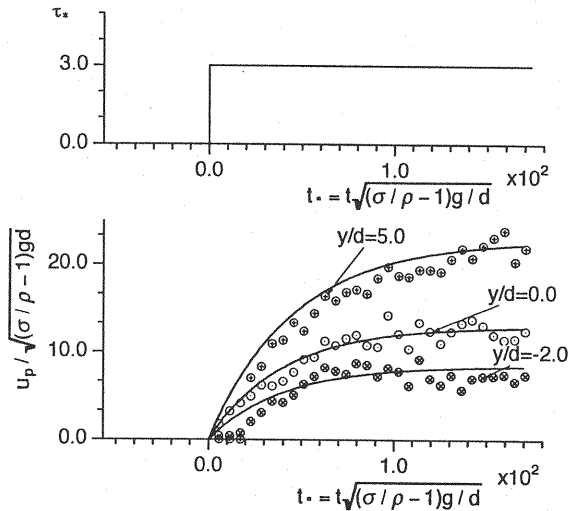


Fig. 2 Accelerating process of particles

at the inter-particle contacting point  $\mu$  ( $=0.3$ ); upper limit of compression force for the elastic behavior of springs  $e_{n\max}$  ( $=2.5$  N),  $e_{s\max}$  ( $=0.025$  N); and the time scale of calculation  $\Delta t$  ( $=1.0 \times 10^{-5}$  s).

### ACCELERATING PROCESS OF GRANULAR-MATERIAL FLOW AS A RELAXATION PROCESS

Figure 2 shows the response of velocity of sand particles to the abrupt change of shear stress acting on the surface of sand layer. Particles do not respond immediately to the change of shear stress, in other words, the motion of particles follows the relaxation process. The development process of vertical profile of particle velocity is shown in Fig. 3. Particle-velocity profile is developing gradually, and approaching to the equilibrium state. At the time  $t_*=5.69$ , or the time just after the initiation of motion, the upward convex profile is maintained. At the time  $t_*=45.49$ , at the upper part, symptom of the shift to vertically uniform distribution can be seen. The upward concave profile in the upper layer, which is the typical profile in the saltation layer, is connected via a inflection point around  $y/d=0.0$  to the upward convex profile in the lower layer. The development of the thickness of sediment-moving layer completes approximately at the time  $t_*=45.49$ .

The solid curve in Fig. 3 is an approximated expression for the fully developed velocity profile as follows:

$$\frac{u_p}{u_{p\inf}} (= \Xi_{up}(y)) = \begin{cases} \alpha \ln\left(\frac{y - y_{\inf}}{d} + 1\right) + 1 & \text{for } y > y_{\inf} \\ \exp\left(\beta \cdot \frac{y - y_{\inf}}{d}\right) & \text{for } y \leq y_{\inf} \end{cases} \quad (4)$$

in which  $u_{p\inf}$ =particle velocity at the inflection point; and  $y_{\inf}$ =elevation of the inflection point. The constants in this equation are determined to accomplish the good agreement with this equation and the developed velocity profile calculated by the DEM as follows:  $\alpha=0.42$ ,  $\beta=0.4$ ,  $u_{p*inf} (= u_{p\inf} / \sqrt{(\sigma / \rho - 1)gd}) = 13.3$ ,  $y_{\inf}/d=0.0$ .

The characteristics of the development of the particle-velocity profile shown in Fig. 2 can be formulated by convolution integral as follows:

$$u_p(t, y) = \Xi_{up}(y) \int_0^{\infty} u_{p\infty}(t - \tau) \bullet T_R(\tau|y) d\tau \quad (5)$$

in which  $T_R(\tau|y)$ =impulse-response function; and  $u_{p\infty}$ =fully developed, or equilibrium, velocity scale, which is unique under the given bottom shear stress. The solid curves in Fig. 2 are time series of particle velocity calculated by applying the impulse-response function as follows:

$$T_R(\tau|y) = \frac{1}{\Gamma(y)} \exp\left\{-\frac{\tau}{\Gamma(y)}\right\} \quad (6)$$

This function shows the satisfactory agreement with the simulated data by adjusting the relaxation scale  $\Gamma(y)$ . In this study, the response of granular material to the abrupt change of the surface-shear stress is treated. The time dependent change of shear velocity follows the step function as follows:

$$u_*(t) = u_{*amp} \bullet \text{He}(t) \quad ; \quad \text{He}(t) = \begin{cases} 0 & \text{for } t < 0 \\ 1 & \text{for } t \geq 0 \end{cases} \quad (7)$$

in which  $u_{*amp}$ =amplitude of shear velocity. The velocity scale, or the velocity at an inflection point, also can be written as

$$u_{p\infty}(t) = u_{p\infamp} \bullet \text{He}(t) \quad (8)$$

in which  $u_{p\infamp}$ =amplitude of particle velocity at an inflection point. By substituting Eqs. 6 and 8 into Eq. 5, the convolution integral can be calculated analytically. Then the velocity profile in the developing

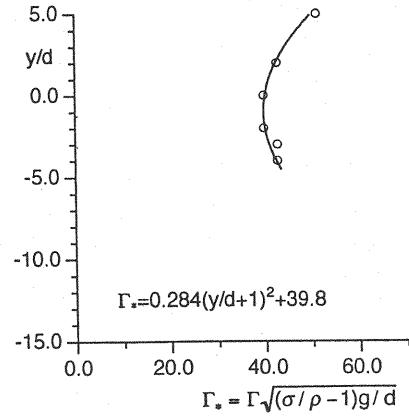
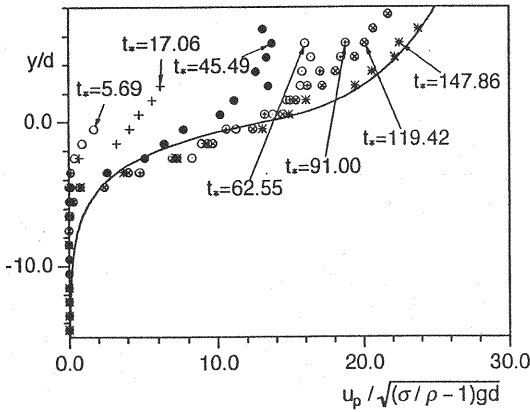


Fig. 3 Development of particle velocity profile Fig. 4 Distribution of relaxation time scale

process can be written as follows:

$$u_p(t, y) = u_{p \text{ inf amp}} \Xi_{up}(y) \left[ 1 - \exp \left\{ -\frac{t}{\Gamma(y)} \right\} \right] \quad (9)$$

Figure 4 shows the vertical distribution of the relaxation scale. Figure 5 shows the comparison between the simulation data of DEM and the calculated curves by the relaxation model. The relaxation model shows the good agreement with the simulation data, hence it can be useful to express the fundamental characteristics of developing process of particle velocity profile.

### MOTION OF INDIVIDUAL SEDIMENT PARTICLE

Figure 6 shows the snapshots of granular material to visualize the instantaneous motion of particle in a developing process of particle-velocity profile. At the time  $t_*=5.69$ , or the time just after the initiation of the action of shear stress, the dispersion of particle is rather small. Few particles in the top part of the moving layer show active motion. This kind of the motion of particle, or the laminar motion, brings the upward convex profile shown in Fig. 3. At the time  $t_*=17.06$ , the dispersion region grows up, then some of the particles in the top layer reach to the elevation around  $y/d=2.0$ . At the time  $t_*=45.49$ , the tendency of the particle dispersion becomes significant, and the dispersion region, or saltation layer, which has been growing up both in upward and downward direction from  $t_*=17.06$  to  $t_*=45.49$ , is spread with the extent of  $-4.0 < y/d < 5.0$ . Although the dispersion region shows the gradual enlargement, even after  $t_*=45.49$ , the primal process of the development of particle-moving layer has almost completed until  $t_*=45.49$ . At the same time, the transition to the particle velocity profile with inflection point also has almost completed. This fact shows that the development of the velocity profile of particle is affected by the development of the dispersion of sediment particle.

Figure 7 shows the number-density distribution of the sediment particle. The solid

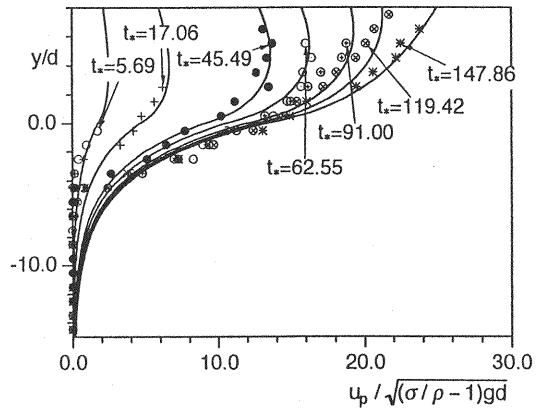


Fig. 5 Relaxation model prediction - comparison between relaxation model and DEM

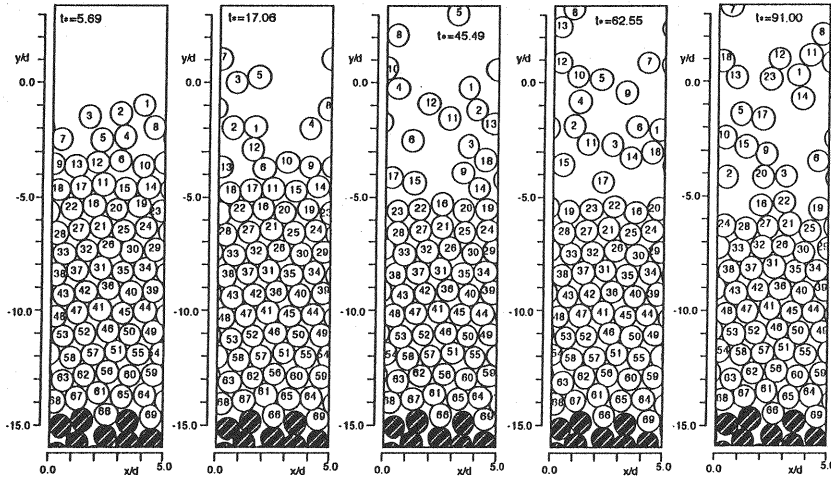


Fig. 6 Instantaneous motion of particles

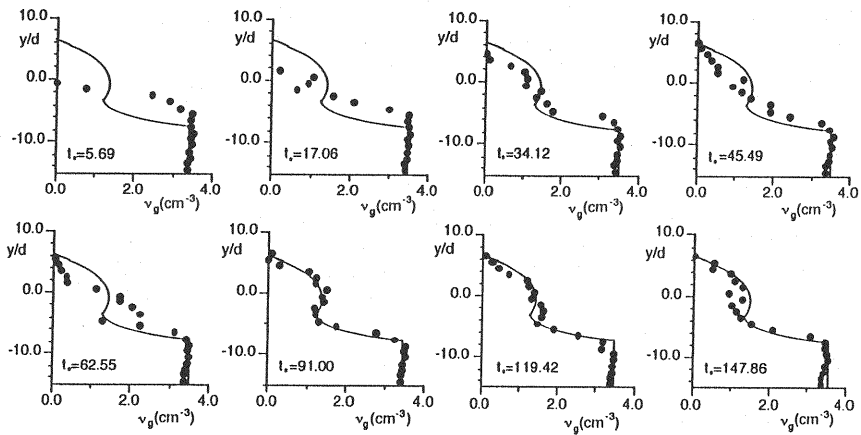


Fig. 7 Development of particle number density

curve in this figure shows the distribution in the equilibrium state, to show the differences between each instantaneous state and the equilibrium one. The existence of the deposition layer, in which the number-density distribution is approximately uniform, is common to all instantaneous distributions. At the time just after the initiation of the action of shear stress, or  $t_* = 5.69$ , the upper edge of the deposition layer is located around  $y/d = -4.0$ . The upper edge of the deposition layer is shifting downward with the development of granular material flow. The upper edge of the number-density distribution, or the upper edge of the particle dispersion region, is also shifting upward with the development of the flow. As it can be seen in Fig. 6, the primal part of the development has almost completed at  $t_* = 45.49$ , and until then the upper part of the number-density distribution exists approximately at the same level  $y/d = 6.0$ . The number density at the equilibrium state gradually decreases upward from the deposition layer ( $y/d < -8.0$ ), and rapidly decreases after showing a small peak around the elevation  $y/d = 0.0$ . The same kind of the peak in number-density distribution was reproduced in the previous numerical simulation of the saltation on fix bed by Gotoh, Tsujimoto and Nakagawa (7). Although the peak in Fig. 7 can be regarded as the same kind of the peak found in the saltation on a fixed bed, the existence of the peak is

rather unclear than that of the saltation on a fixed bed. This characteristics can be attributed to the uncertainty of the elevation of the bottom boundary in movable bed, because of the frequent deformation of the arrangement of bottom constituting particles of movable bed.

## CONCLUSION

In this study, behavior of granular material under a sudden change of the shear force acting on the surface is investigated by using a simulation based on the DEM. The development process of the velocity profile of the sand particles shows the same characteristics as the relaxation process, therefore a relaxation model, which has the convolution integral formulation, is applied to express the development process of the particle velocity profile. Detailed motion of the particles is investigated through the continuous frames of the snapshots of moving particles. The number density distribution is also estimated from the calculated result of DEM. Through the snapshots and the number density distribution, the mechanism of the developing granular material flow is discussed from a view point of the particle/particle interaction.

## ACKNOWLEDGMENT

The authors wish to express their gratitude to Messrs. Y. Toyota and A. Sakai (former Graduate Students, Kyoto Univ.) for their help with the data processing.

## REFERENCES

1. Gotoh, H., Sakai, T. and Tominaga, K.: Numerical Simulation of Sheetflow based on Distinct Element Method, *Proc. Coastal Eng., JSCE*, Vol. 41, pp. 371-375, 1994 (in Japanese).
2. Gotoh, H. and Sakai, T.: Numerical Simulation of Sheetflow as Granular Material, *Jour. of Waterway, Port, Coastal and Ocean Engrg., ASCE*, Vol. 123, No. 6, pp.329-336, 1997.
3. Cundall, P. A. and Strack, O. D.: A Discrete Numerical Model for Granular Assemblies, *Geotechnique*, Vol. 29, No. 1, pp.47-65, 1979.
4. Oda, K., Shigematsu, T. and Ujimoto, K.: Descent and Dispersion Analysis of Dumped Particles in Water by Means of a Combined DEM-MAC method, *Liquid-Solid Flows-1991*, pp. 159-163, 1991.
5. Mishima, M., Akiyama, S. and Tsuchiya, Y.: Numerical Study of Grain-Bed Impacts in Blown Sand, *Proc. Coastal Eng., JSCE*, Vol. 40, pp. 271-275, 1993 (in Japanese).
6. Haff, P. K. and Anderson, R. S.: Grain Scale Simulation of Loose Sedimentary Beds: - The Example of Grain-Bed Impacts in Aeolian Saltation, *Sedimentology*, Vol. 40, 175-198, 1993.
7. Gotoh, H., Tsujimoto, T. and Nakagawa, H.: Numerical Model of Interphase Momentum Transfer and Interparticle Collision in Bed-Load Layer, *Proc. APD-IAHR*, Singapore, pp. 565-572, 1994.

## APPENDIX-NOTATION

The following symbols are used in this paper:

$d$	= diameter of particle;
$e_{n\max}, e_{s\max}$	= the upper limit of the compression force acting on the spring;
$F_{oi}$	= shear force acting on the $i$ -th particle;
$f_n, f_s$	= normal and tangential components of the force acting between particles on the local coordinate system $n$ - $s$ ;
$g$	= gravitational acceleration;
$I$	= moment of inertia of particle;
$k_n, k_s$	= spring constants in the normal and tangential direction;
$M$	= mass of particle;
$r$	= radius of particle;
$t^*$	= dimensionless time scale ( $= t\sqrt{(\sigma/\rho-1)g/d}$ );
$T_R$	= impulse-response function of particle velocity;

$u_p$	= velocity of the particle in streamwise direction;
$u_{inf}$	= particle velocity at an inflection point of velocity profile;
$u_{pinfamp}$	= particle velocity amplitude at an inflection point of velocity profile;
$u_*$	= dimensionless shear velocity;
$u_{*amp}$	= amplitude of the dimensionless shear velocity;
$V$	= volume of the particle;
$x_i, y_i$	= coordinate of center of $i$ -th particle in streamwise and upward vertical direction, respectively;
$y_{inf}$	= elevation of inflection point of velocity profile;
$\alpha, \beta$	= constants of approximated expression of equilibrium particle velocity profile;
$\alpha_{ij}$	= contacting angle between the $i$ -th and $j$ -th particles;
$\Gamma$	= relaxation scale of particle velocity;
$\Delta t$	= time step for calculation;
$\eta_n, \eta_s$	= damping coefficients in the normal and tangential direction;
$\mu$	= coefficient of friction;
$\phi_i$	= rotating angle of $i$ -th particle;
$\rho$	= mass density of fluid; <i>and</i>
$\sigma$	= mass density of particle.

(Received April 24, 1997; revised March 27, 1998)